

Updates to the AMSR-E V05 Algorithm

February 7, 2006

1. Introduction

A major update to the AMSR-E processing algorithm was completed February 6, 2006. This update is called Version 5 (V05). This document describes the changes that were made relative to the previous Version 4 (V04). The changes are summarized below and further details are given.

Summary of changes:

1. Improvements to the geolocation routines have been made. The latitude and longitudes for the geophysical retrievals are now more accurate. Errors in V04 were as large as 5-10 km. For V05 the error is estimated to be 1 to 3 km.
2. A correction has been applied to remove moon contamination in the AMSR-E cold mirror.
3. Improvements have been made to the AMSR-E rain rates, with an overall effect of reducing the rain rates substantially in the tropics.
4. Near-real time bytemaps and imagery that is 3 to 6 hours behind real time are now available. This represents a decrease in data latency of 12 to 16 hours relative to the V04 products.

2. Changes to Geolocation Routines

We and others have recognized for some time that the AMSR-E brightness temperature imagery was misregistered relative to coastlines and other land features. The error in geolocation was about 5-7 km and could be as large as 10 km. The misregistration was most apparent when differencing ascending imagery and descending imagery. The ascending imagery was shifted one way and the descending imagery was shifted the other way, thereby making the problem more apparent. Figure 1 shows an example.

After some analysis, it was recognized that the misregistration was due to a misalignment of the AMSR-E sensor relative to the spacecraft. This problem was fixed by a trial-and-error method in which various roll, pitch, and yaw corrections were applied to the AMSR-E alignment until proper registration was obtained. This was done by two completely independent analyses. The first analysis was done by Peter Ashcroft of RSS using the island of Kauai as a reference. The AMSR-E alignment was varied until the imagery of Kauai was co-registered with a high-resolution map of the Kauai coastline. The second analysis done by Frank Wentz relied on the ascending-minus-descending imagery like that shown in Figure 1. Left-swath minus right-swath imagery was also used. Proper alignment is obtained when the halo-like effects near coastlines, rivers, and other high-contrast land and ice features go away as shown in Figure 1. Both analyses resulted in nearly the same set of adjustment parameters. A comparison of the two different approaches suggests that the accuracy of the geolocation analysis is between 1 and 2 km, which is the accuracy we now place on the AMSR-E cell locations.

A separate geolocation analysis was done for each channel (14 in all). The results show that for a given frequency the v-pol and h-pol channels are well aligned. Furthermore, the 19, 23, and 37 GHz channels are also well aligned with each other. Table 1 gives the azimuth, cone, and roll angles that are required at each frequency to achieve proper geolocation.

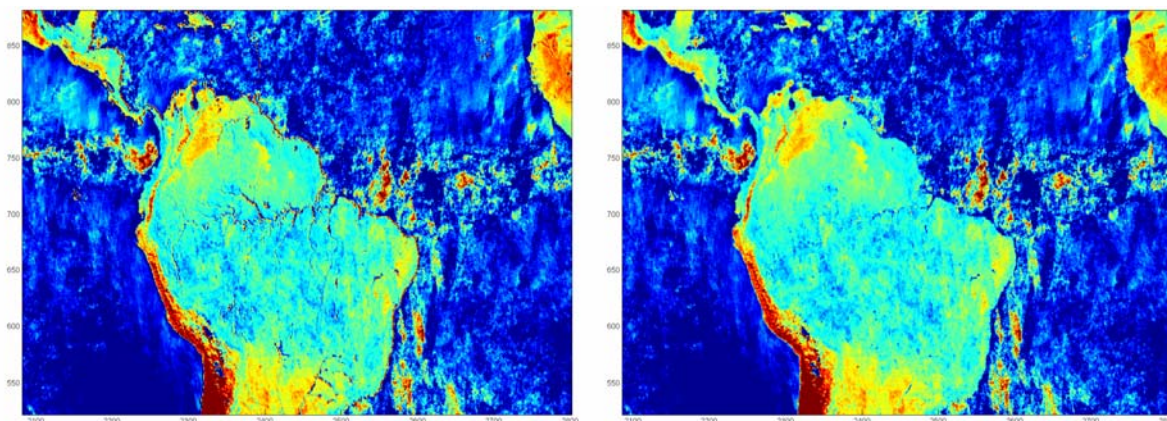


Figure 1. An ascending minus descending difference map of AMSR-E 37-GHz imagery. In the left image you can see a halo effect near coastlines, rivers and other land features having a sharp contrast. The right image is obtained after applying corrections to compensate for the AMSR-E misalignment.

Table 1. The Alignment Angles for AMSR-E Deduced from the Geolocation Analysis

Channel	Azimuth angle (deg.)	Cone angle (deg.)	Roll angle (deg.)
7 GHz	-74.838	47.67	0.09
11 GHz	-74.948	47.64	0.09
19 GHz	-74.948	47.57	0.09
24 GHz	-74.948	47.57	0.09
37 GHz	-74.948	47.57	0.09
89 GHz A	-75.148	47.57	0.09
89 GHz B	-75.424	47.09	0.09

3. Resampling 7 and 11 GHz channels to Match Locations for Higher Frequencies

The geolocation analysis already discussed showed that the 7-GHz and the 11-GHz horns are pointing in slightly different directions than the 19, 23, and 37-GHz horns. Rather than providing a separate set of latitudes and longitudes for 7 GHz and another set of 11 GHz, we decided it would be more useful to resample the 7 and 11 GHz observations in such a way as to match the location of the higher frequencies. Since these channels are being resampled anyway, it makes sense to adjust the resampling weights so that the resampled T_A at 7 and 11 GHz match the location of the higher frequencies. This required rederiving the sampling weights, this time

with the center of the target cell positioned at the location of the 19 GHz channel rather than at the 7 or 11 GHz footprint position. One drawback to this is that the un-resampled 7 and 11 GHz observations are missing an exact specification of latitudes and longitudes. Figure 2 gives an example of the improvement.

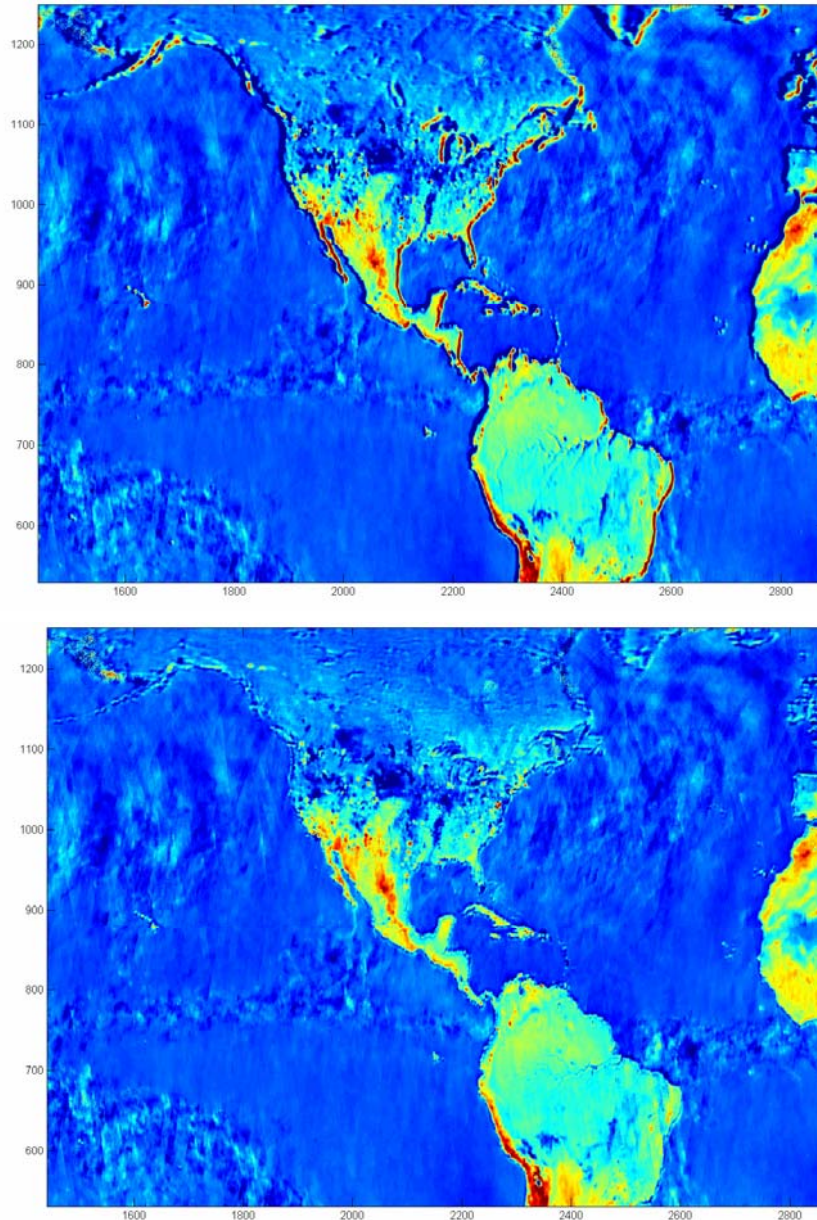


Figure 2. An ascending minus descending difference map of AMSR-E 7-GHz imagery. The top image is with the old geolocation parameters and the old resampling weights that did not adjust the location of the imagery. The bottom image is with the new geolocation parameters and the new resampling weights that align the 7-GHz imagery with the 19-GHz imagery. Notice the reduction in the halo effect near coastlines, rivers and other land features in the bottom image.

4. Implementation of Using UT1 Time to Compute the Earth Rotation Angle.

Aqua's position, velocity, and attitude vectors are given in terms of the J2000 inertial coordinate system. To compute Earth latitudes and particularly longitudes, it is necessary to compute the Earth rotation relative to the J2000 systems. The proper calculation requires using the UT1 time, which can be as much as one second different from UTC time. To obtain UT1, the L2A algorithm now accesses U.S. Naval Observatory database each day to obtain the current UT1. One advantage of this procedure is that it is independent of leap seconds. That is to say, there is no discontinuity in the geolocation parameters when a leap second occurs.

5. Correction for Lunar Radiation Entering the AMSR-E Cold Mirror

Twice each month the moon enters the field of view of the AMSR-E cold mirror. The Moon's surface temperature varies from 120 K at night to 370 K in the day and has a relatively high emissivity. As a result, the moon acts as a source of contamination to the cold sky measurement.

A correction is applied to remove the lunar contamination. The correction depends upon the following factors:

- a. The angle between the vector going from the satellite to the moon and the boresight vector of the cold mirror. This is the dominant term. When this angle becomes small (a few degrees or less), lunar contamination become significant. This angle is called the lunar angle.
- b. The phase of the moon. A full moon is hotter than a new moon and hence has a higher brightness temperature.
- c. The distance from the satellite to the moon. Radiation intensity falls off as the inverse of the square of the distance.

The lunar T_A contribution to the cold sky observations is computed and then is scaled in terms of cold counts. The 'lunar cold counts' are subtracted from the AMSR-E cold count observations to obtain a cold count value free of lunar contamination. For the case of 89 GHz, when the lunar angle is less than 1° , the lunar contamination is too large to perform the correction, and these observations are flagged as bad and are not processed. The excluded observations are extremely rare. The accuracy of this correction is estimated to be of the order of 0.1 K.

6. Improved Rain Algorithm

We re-derived the relationship between rain column height and sea surface temperature using NCEP freezing level heights in raining conditions. The new relationship produces freezing level heights that are much more realistic and spatially representative. In addition, we have made two major changes to the beamfilling correction. 1) Previously, we allowed the correction to "max-out" when the radiometer saturated. The new correction produces more realistic corrections when saturation occurs. 2) We now incorporate footprint size into the beamfilling correction in order to bring AMSR-E rain rates into better agreement with rain rates from other microwave radiometers. Due to the revised freezing level height, rain rates from the new algorithm are substantially lower in the tropics.

7. Near-Real Time Bytemaps and Imagery

A new near-real time product (RT) is now being provided in addition to the final product. The RT products are contained in the bytemaps with the suffix "rt". The final products are contained in the bytemaps with the suffix "v5". Typically for the current day, the RT bytemaps will contain geophysical retrievals that are about 12-16 hours fresher than in the V5 bytemaps. The RT data will be between 3 and 6 hours behind real time. The browse imagery on our website now shows the RT bytemaps rather than the V5 bytemaps for the most current two days. The RT bytemaps and imagery are only kept for 2 days, at which point the final V5 results replace them. The accuracy of the RT data is not as high as the final V5 data, but it should be suitable for data assimilation, forecasting, and other near-real time applications. Climate studies should still be based on the final V5 data.